www.adeepakpublishing.com

Aheieva, K. et al. (2021): JoSS, Vol. 10, No. 2, pp. 1035–1048
(Peer-reviewed article available at www.jossonline.com)

www. JoSSonline.com

Project Overview of SPATIUM-I: A Technology Demonstration Mission Toward Global Three-Dimensional Ionosphere Mapping via CubeSat Constellation Equipped with an Atomic Clock

Kateryna Aheieva, Rahmi Rahmatillah, Ryotaro Ninagawa, Ibukun Owulatobi Adebolu, Sangkyun Kim, Yuta Kakimoto, Takashi Yamauchi, Hirokazu Masui, and Mengu Cho
Kyushu Institute of Technology
Kitakyushu-shi, Fukuoka-ken, Japan

Chow Chee Lap, Zhang Ying, Tse Man Siu, Li King Ho Holden, and Mengu Cho
Nanyang Technological University
Singapore

Abstract

Many satellites currently measure ionosphere density in low Earth orbit (LEO), yet this information remains insufficient to create a global three-dimensional ionosphere map. Because the ionosphere constantly fluctuates on a global scale, to improve and validate existing ionosphere models, simultaneous measurement of the electron density at the global scale is necessary. To measure the total electron content (TEC) and have higher spatial and temporal resolution, higher accuracy, and a lower cost than the Global Navigation Satellite System (GNSS), the current study proposes a CubeSat constellation equipped with a UHF inter-satellite ranging payload. With 1,000 satellites on different orbital planes in LEO, we can achieve a horizontal spatial resolution of 20 km and a temporal resolution of 15 min. The electron density distribution can be known by solving the inverse problem from many observations provided by the constellation.

The first pathfinder satellite, SPATIUM-I, was released from the International Space Station (ISS) on October 6, 2018. SPATIUM-I will validate the Chip-Scale Atomic Clock (CSAC), a commercial off-the-shelf (COTS) atomic clock, and other key technologies in orbit. The project was jointly developed by the Kyushu Institute of Technology in Japan and Nanyang Technological University in Singapore. This paper will provide an overview of the SPATIUM-I mission and its satellite system.

Corresponding Author: Kateryna Aheieva – katerynaheieva@gmail.com
Publication History: Submitted – 03/01/2020; Revision Accepted – 06/08/21; Published – 07/10/21

1. Introduction

The ionosphere constantly fluctuates on a global scale, causing disturbances in the ionosphere that can affect aspects of daily life such as radio communication, navigation, etc. Ionospheric variability is strongly controlled by perturbations in the neutral atmosphere, electrodynamics, solar activity, and geomagnetic activity. Gravity waves and localized electric fields, such as transient luminous events, can also result in small-scale variability in ionospheric density at certain regions. If we can reconstruct global three-dimensional (3D) ionospheric density, it will help us to better understand the ionospheric morphology and its perturbations, as well as providing us with more information to investigate the sources of these variabilities.

Currently, to ascertain how the ionosphere changes globally in time, we rely on numerical simulations. State-of-the-art models, such as the Ground-to-Topside model of the Atmosphere and Ionosphere for Aeronomy from NICT out of Japan (ISEE, no date) and the coupled Whole Atmosphere Ionosphere Model and Ionosphere Plasmasphere Electrodynamics Model from the US National Oceanic and Atmospheric Administration (NOAA, no date), can simulate ionosphere variability due to perturbations from the lower atmosphere and solar activity, as well as from geomagnetic activity. Measurement by individual satellites helps to validate and improve the models, but observation alone cannot reveal how the 3D structure of the ionosphere changes globally in time.

Time-varying global 3D structure of the ionosphere based on observation by constellation satellites alone will provide extremely valuable information to improve the ionosphere models and greatly advance our knowledge of coupling among the Sun, magnetosphere, ionosphere, atmosphere, and the Earth. Incorporating the measurements into these models with data assimilation techniques, space weather forecasting capability can be significantly improved.

At present, it is possible to know the total electron content (TEC) and total precipitable water (TPW) in a vertical direction by measuring the phase of the ranging signals or the carrier waves from Global Navigation Satellite System (GNSS) satellites on the ground. It is also possible to know the vertical electron density distribution with 100 m resolution using Global Positioning System Radio Occultation (GPSRO) or using a GPS receiver onboard a satellite, although its horizontal resolution is over 100 km. If we limit the target to only the area above the ground station (GS), combining the two measurements (the phase of the ranging signal and signal delay), it is possible to derive a 3D ionosphere density distribution.

However, if we use GNSS signals, it is difficult to perform global 3D mapping with enough accuracy and temporal/spatial resolution. GNSS signals have two main limitations. The first is the fact that the GNSS frequency (the L-band) was chosen so that radio wave propagation would not be affected much by the ionosphere and atmosphere, making measurement less precise. The second is the fact that the GNSS orbit altitude is very high. Hence, TEC contains a contribution of plasma over very long distances. The radio wave propagation delay is inversely proportional to the square of the frequency. Using a lower frequency such as UHF and inter-satellite ranging among LEO satellites will lift these limitations.

The final goal of the research is to do global 3D ionosphere mapping via a CubeSat constellation equipped with an atomic clock. The target is to have 20-km horizontal resolution and 15-min temporal resolution using inter-satellite ranging via UHF signals among CubeSats in LEO. The total targeted program cost is 250 million USD ($180 million for launch, $50 million for satellite hardware, $15 million for personnel, and $5 million for GSs) for a three-year operation in orbit. That total cost is half that of the COSMIC-2 project, which cannot do global simultaneous mapping. Because the proposed system uses UHF signals (467 MHz assumed) among LEO satellites, the horizontal and temporal resolution improves by one order of magnitude compared to the case where the L-band GNSS signal is used (the difference between L-band 1.3 GHz and UHF band 467 MHz frequencies square).

We can now acquire a precise commercial off-the-shelf (COTS) chip-scale atomic clock (CSAC) small enough to be housed in a CubeSat and accurate enough to provide a clock signal to measure the radio wave propagation delay. The frequency stabilization is 10^{-10} in one second, which is sufficient to derive TEC even with the carrier wave phase delay.

Since 2016, the Kyushu Institute of Technology (Kyutech) in Japan and Nanyang Technological University (NTU) in Singapore have been jointly developing a 2U CubeSat, SPATIUM-I, to validate some of the key technologies in orbit. The satellite was launched to the International Space Station (ISS) in September 2018. The satellite was released from the ISS in October 6, 2018.

The SPATIUM-I missions are as follows:

1. In-orbit demonstration of CSAC;
2. In-orbit demonstration of spread-spectrum (SS)-modulated 467-MHz Tx with CSAC as a clock source;
3. In-orbit demonstration of 401-MHz Tx and Rx for the second UHF band;
4. Demodulation of SS signal on the ground;
5. Time synchronization of multiple GSs (via GPS and CSAC clocks); and
6. Reading the carrier wave phases (401 MHz and 467 MHz) of a single satellite.

Once SPATIUM-I is successful in those missions, we plan to launch SPATIUM-II, the next technology demonstration toward SPATIUM-III. SPATIUM-II will be a constellation consisting of eight 3U CubeSats, and will perform an in-orbit validation of all nine technology items listed above, for SPATIUM-III.

The final operational system (SPATIUM-III constellation) will be made of 1,000 3U CubeSats in nine orbital planes in LEO. The satellite altitudes are made of three layers below 550 km, to provide the full coverage and continuous intersatellite communication and deorbit satellites within the required 25 years (for satellites on LEO orbits). Each satellite will carry a GNSS receiver to know its location when the signals are transmitted or received. In addition, each will carry a double Langmuir probe (DLP) to measure the plasma density in situ, and each will continue transmitting the UHF ranging signal (467 MHz) in all directions. The signal is spread-spectrum (SS) modulated, so that multiple satellites can simultaneously share the single frequency. Each satellite will carry a UHF receiver to demodulate the ranging signal. The ranging signal contains data that identifies the satellite and expresses the time, satellite position, plasma density, etc. Figure 1 shows a conceptual picture of the SPATIUM-III constellation.

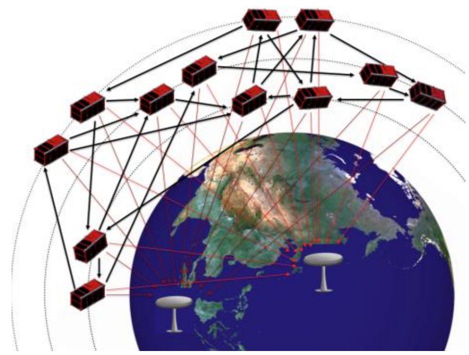

Figure 1. Conceptual picture of the SPATIUM-III constellation.

A satellite at a 500-km altitude can see up to 5,000 km in the horizontal direction. The RF output power of 1W is enough to communicate over this distance.

By exchanging the ranging signals in SPATIUM-III constellation, each satellite derives the TEC along the inter-satellite path. The TEC and the in situ plasma density data will be processed onboard. With a rate of ten measurements per second between satellites, we can acquire four million data in 30 minutes. The data packet (a minimum of 116 bits per measurement) will be downlinked to the GSs. The inverse problem will be solved on the ground to derive the 3D plasma density distribution. Approximating the electron density vertical profile by a function with ten independent parameters, we can obtain the density distribution with a 20-km horizontal resolution. The UHF radio wave path length becomes 100 m longer for 500-km propagation with an electron density of $10^{12}m^{-3}$. If we can identify the satellite location within the position knowledge of 1 m (standard deviation σ, and the approximated satellites and GS location coordinates), we can derive TEC with sufficient accuracy. In conclusion, we can derive the 3D global plasma density distribution of a spherical shell between the ionosphere bottom and a 550-km altitude with a temporal resolution of 15 minutes. The horizontal spatial and temporal resolutions of 20 km and 15 min are good enough to reveal the motion of a plasma bubble whose size is ~100 km (Barros et al., 2018) and moving with a speed of ~100 m/s (Huang et al., 2011).

To realize the SPATIUM-III constellation, the following technical necessities must be achieved:

1. CSAC working correctly in the space environment;

2. SS-modulated UHF transmitter onboard a CubeSat;
3. SS-modulated UHF receiver onboard a CubeSat;
4. Satellite positioning within an error of 1 m or less;
5. In situ plasma measurement by a CubeSat;
6. Operation of CubeSat constellation;
7. Derivation of TEC and TPW from the phase differences of ranging signals and carrier waves among multiple GSs;
8. Derivation of TEC between satellites; and
9. Derivation of 3D plasma density distribution.

The purpose of this paper is to describe the SPATIUM-I project, its mechanical and electrical design, all project difficulties met during the design and testing phase, changes that were made to be able to fulfill the requirements listed above, and main mission specification and communication validation for continuous data transmission to the GSs in terms of power and link budgets. This paper is written to serve as a reference for future CubeSat projects to perform a mission similar to that of SPATIUM-I for clock signal broadcasting and various observations and measurements using CSAC.

The current paper comprises five parts. The second part describes the SPATIUM-I satellite mechanical and electrical design, mission configuration, data content, communication principles, satellite link budget, difficulties we had during the development phase, and their solutions. The third part describes the SPATIUM-I GS, equipment, and the principles of data analysis. It also describes the amount of data we can receive using SPATIUM-I and the benefits for SPATIUM-III projects. The fourth part describes the initial status of the satellite operation, and the fifth part presents our conclusions for all the work that was done during the satellite development.

2. SPATIUM-I Satellite

The SPATIUM-I satellite is a 2U CubeSat (Figure 2), developed based on the bus system of the BIRDS project satellite (Tejumola, 2017; Tokunaga, 2017). The satellite contains an electric power system (EPS) and communication system (COM) that play a partial role in the onboard computer (some of the simple satellite control will be done by the microprocessor on the COM), and a main mission board, that we call the CSAC board. The CSAC board consists of two boards connected together and represents one system. The first board includes the CSAC (Microsemi QuantumTM SA.45s CS) itself with a 10-MHz frequency output, and the second board carries supercapacitors with a total capacitance of 90F.

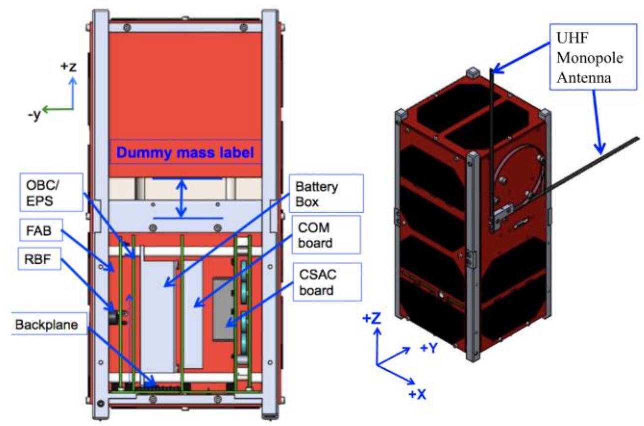

Figure 2. The SPATIUM-I satellite design.

Originally, SPATIUM-I was designed as a 1U CubeSat (Aheieva et al., 2017a). For mission success and continuous data reception, analysis and storage, one of the requirements for the COM was continuous data transmission from the satellite to the GS. This will help store the CSAC counter data from the beginning of the satellite operation, right after its release from the ISS. While a power generation profile showed that continuous transmission would require higher power (about 1.8 W, even with a 20% duty cycle for only the COM board), the satellite shape was changed to a 2U CubeSat.

SPATIUM-I has no active or passive attitude control system. Under the limited satellite operation/transmission time of 20% duty cycle, the satellite already has limited, but adequate energy to support an active orientation system. Permanent magnets were removed to simplify the satellite design and to remove any possible disturbance to the main CSAC mission. For the first satellite and a demonstration mission, the satellite orientation was considered insignificant in comparison with the need to confirm the mission's success.

The 2U system can generate 2.3 W of power, using 18 solar cells, and stores it in 2000 mAh nickel–metal hybrid batteries. Continuous satellite operation requires 2.25 W, on average. For extra mission support, we are using a supercapacitor that could drive the CSAC board for around 20 minutes, while the battery is charging. This countermeasure will guarantee continuous counting of the 10-MHz signal.

The system is designed in such a way that, if a power blackout occurred due to any unexpected situation (e.g., longer eclipse time due to low beta angle), the satellite, after recovery-battery charging, will start transmission from its initial state, in nominal mode (same as after its first release from the ISS). The nominal mode for the SPATIUM-I satellite is a continuous transmission with a 20% duty cycle: 2-min transmission is ON and 8-min transmission is OFF.

The system has two independent counters: a CSAC board counter and a COM board counter. The data from both are the same. The COM board counter is the main counter that collects the 10-MHz signal data, which is received from the CSAC. The CSAC board counter is a back-up counter in case the COM board briefly stops operation due to emergency. The CSAC board counter data go to the COM board main processor and are transmitted to the GS together with the COM counter, so we can compare the results.

If the battery becomes over-discharged, the CSAC board will get power support from its own supercapacitor system with a capacitance of 90F and will be able to continue counting and storing data to the CSAC board counter's memory, while the COM counter loses power. The COM board will be able to transmit this data if the battery voltage recovers. Usually, a satellite battery can charge up to 4.2–4.3 V and a CSAC board supercapacitor has a voltage level of around 4.2 V. When the satellite battery voltage drops down to 3.1–3.2 V (Figure 3, line 1), the CSAC board starts to use power from the 90F supercapacitor (due to a voltage limitation on the components placed between the EPS and CSAC board supercapacitor). If the battery voltage becomes lower than 2.3–2.4 V, the COM board cannot continue data counting and stops transmission due to the low power (Figure 3, line 2). The supercapacitor can support CSAC operation until it discharges to ~2.6–2.8 V (Figure 3, line 3). If the supercapacitor voltage is lower than 2.6 V, the CSAC board cannot count and transmit the 10-MHz data anymore. The next transmission after recovery will start from the initial state and zero counts on both counters (Figure 3, line 4).

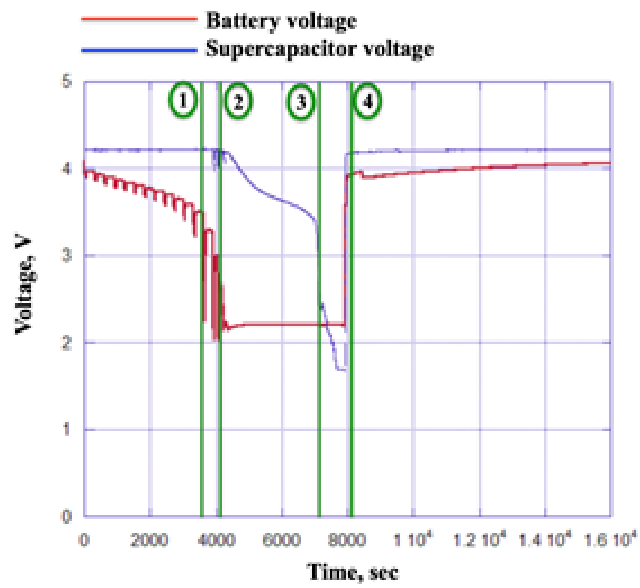

Figure 3. SPATIUM-I power system operation.

To simplify the satellite bus, it was decided to remove the main onboard computer (OBC). We plan to downlink the housekeeping (HK) data only if necessary and from time to time, using a command from the GS. The main mission data (counter value of 10-MHz CSAC clock signal) will be transmitted from the CSAC board to the COM board microprocessor, modulated with a PRN code, and will be transmitted to all network GSs that have the same reference CSAC, as on-board the satellite and GPS clocks (for GS synchronization).

SPATIUM-I uses two frequencies for downlink: 467 MHz and 401 MHz. With both frequencies, we can receive the main mission data (CSAC 10-MHz counter) and HK data. The difference is in the content of the HK data (points 6, 7 and 8 listed below).

The 467-MHz frequency carries the following data in one packet:

1. Sync marker: 24 bits "FAF320"
2. Spacecraft ID: 8 bits
3. Operation mode: 8 bits

4. Flame counter: 56 bits
5. CSAC counter: 64 bits
6. Internal CSAC temperature: 16 bits
7. UNREG PWR voltage: 16 bits
8. RSSI: 16 bits
9. BAT temperature: 16 bits
11 COM temperature: 16 bits
12. Command increment counter: 8 bits
13. Other: 2 bits reserved

Total (1-13): 250 bits

The 401-MHz frequency was assigned packet data as follows:

1. Sync marker: 24 bits "FAF320"
2. Spacecraft ID: 8 bits
3. Operation mode: 8 bits
4. Flame counter: 56 bits
5. CSAC counter: 64 bits
6. CSAC temperature: 16 bits
7. CSAC supercapacitor voltage: 16 bits
8. COM current: 16 bits
9. BAT temperature: 16 bits
11. COM temperature: 16 bits
12. Command increment counter: 8 bits
13. Other: 2bits reserved

Total (1-13): 250 bits

Both frequencies, 467 MHz and 401 MHz, can perform transmissions. The 401-MHz frequency is also used to uplink the command to the satellite.

The 467-MHz downlink frequency uses SS modulation and the biggest advantage is that a satellite constellation will be able to share the same frequency.

The 401-MHz downlink frequency uses Phase modulation (PM), as it is widely used for transmitting radio waves and can also be used in determining the velocity of a moving target by extracting Doppler information. This frequency is also used as the uplink frequency for SPATIUM I with frequency modulation (frequency shift keying, FSK). The frequency modulation technique has a lower probability of error and a high signal-to-noise ratio (SNR).

The 467-MHz downlink frequency uses SS modulation so that future satellite constellations will be able to share the same frequency. The transmission power for this frequency is below 0.5 W for SPATIUM-I.

Table 1. SPATIUM-I Antenna Test Results[a]

Test configuration	Patch antenna	Monopole antenna
467 MHz horizontal	-75	-110
467 MHz vertical	-71	-104
401 MHz horizontal	-78	-108
401 MHz vertical	-82	-104
401 MHz uplink	not measured	-61

[a] Maximum attenuation value when the communication was possible is shown in dB.

The signal bitrate of 467-MHz is 250 bps. The SS modulation is done with a chip rate of 62.5 kHz; therefore, each bit is made of 250 chips.

The two operation frequencies required two different antennas. At the initial satellite design state, we planned to use non-deployable antennas to avoid the risk of deployment and system complexity (Aheieva et al., 2017b). Preference was given to the patch-type antenna because of its simplicity. Each antenna works on its own frequency, 467 MHz or 401 MHz. Each antenna should be connected to +Y and –Y satellite panels (see Figure 1), and each panel should have only three solar cells instead of four solar cells, to provide space for antennas. The total number of solar cells was 18. In the preliminary design, anticipating the use of the patch antenna, we decided to remove the OBC because the satellite operation was a continuous radio emission. The uplink command was only for changing the radio emission modes, which could be handled directly by a processor embedded in the satellite receiver.

For each antenna, we measured the maximum achievable attenuation when the downlink or uplink could be successful in an anechoic chamber where the satellite and antenna receiver were separated by 3.5 m, corresponding to the free space loss of ~36.7 dB). We varied the value of the variable attenuator by an increment of 2 dB to see whether communication was possible or not at each attenuation value. Along with the patch antennas, we also tested deployable monopole antennas. Table 1 lists the maximum attenuation value at which communication was possible. The values listed do not include a free space loss value (for the satellite on 400 km altitude the losses is ~36.7 dB or 3.5 m). The result indicated that patch antenna performance is worse than deployable monopole antenna performance by 20 dB or more. Even taking into account its reliability (no deployment failure), because of this significant performance difference, we decided to use the deployable monopole antennas.

Using data from Table 1, we calculated the link budget for SPATIUM-I uplink and downlink frequencies, using the following equations:

$$M = P_{R_x calculated} + G_R - S_{R_x test} \quad \text{and} \tag{1}$$

$$S_{R_x test} = P_{out} - L_{cable} - Att_{test} \ , \tag{2}$$

where M is the margin, $P_{Rxcalculated}$ is the power received at the GS antenna (Equation 3), GR is the GS antenna gain (19 dBi for the present case) for the downlink and the satellite antenna gain (0.44 dBi for the present case) for the uplink, S_{Rxtest} is the receiver sensitivity from the test, L_{cable} is the cable loss (1.2 dB is assumed), and Att_{tes} is the maximum attenuation level measured during the test (from Table 1). Pout is the power output from the transceiver during the test, and is equal to -13.5 dBm. In Eq. 3, the equivalent isotropically radiated power (EIRP) from the radiated antenna is -3.57 dBm for the downlink and 29 dBm for the uplink. The sum of the transmitter loss, $L_{Txpointing}$, the polarization loss, $L_{polarization}$, and the receiver pointing loss, $L_{Rxpointing}$, is assumed to be 4 dB. The free space loss (FSPL) is 147.67 dB for 401 MHz and 149 dB for 467 MHz for the case of lowest elevation angle (10º) and 136.55 dB for 401 MHz and 137.87 dB for 467 MHz for the case of 90º elevation.

$$P_{R_x calculated} = EIRP - L_{T_X pointing} - L_{polarization} - L_{R_X pointing} - L_{cable} - FSPL \tag{3}$$

For the downlink at the 467-MHz frequency, the satellite will have a 16-dB margin at the lowest elevation angle and a 27-dB margin at the highest elevation. For the antenna at the 401-MHz frequency, the downlink has a 12-dB margin and 24-dB margin for the lowest and highest elevation angles, respectively (Eq. 1 and Eq. 2). If we could not reach the uplink with the patch antenna, we got margins of 2.21 and 13.33 dB (for lowest and highest elevation angle, respectively) on the 401-MHz uplink frequency with the monopole antenna. All data described above are presented in Table 2.

Table 2. SPATIUM-I Link Budget

Frequency	**401 MHz**	**467 MHz**
FSPL, low elevation angle=10deg	147.67	149
FSPL, high elevation angle=90deg	136.55	137.87
GS antenna gain downlink	19 dBi	19 dBi
GS antenna gain uplink	0.44 dBi	0.44 dBi
L_{cable}	1.2 dB	1.2 dB
P_{out}	- 13.5 dBm	- 13.5 dBm
EIRP	29 dBm	3.57 dBm
$L_{Txpointing}$, $L_{polarization}$, $L_{Rxpointing}$	4 dB	4 dB
Margin low elevation angle=10deg	16 dB	12 dB
Margin high elevation angle=10deg	27 dB	24 dB

Monopole antennas have a disadvantage compared with patch antennas, namely, a deployment mechanism. SPATIUM-I antennas are tightened and fixed by fishing line, as shown in Figure 4. To burn the fishing

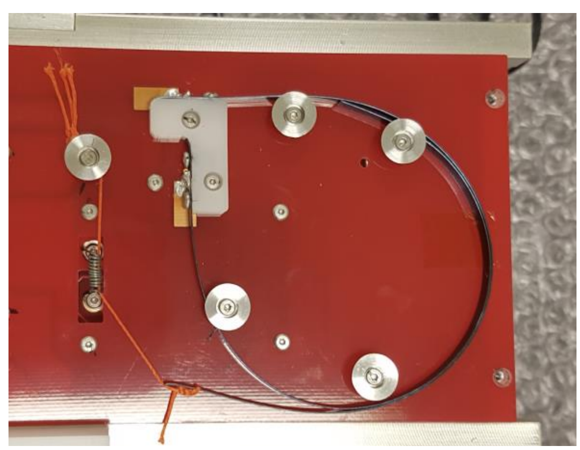

Figure 4. SPATIUM-I antenna's fixation.

line and deploy the antennas, there is a need to supply and control the power to the burner mechanism. The burner circuit shall be operated 30 minutes after the satellite is released from the ISS, due to safety requirements. Also, there may be a need to try the deployment several times if the first attempt fails. Then, there is a need to add something more sophisticated than a simple relay. Because the OBC system was removed, we needed to add a microprocessor to control the power. The power system also needed rerouting. The change from the patch antenna to the monopole antenna cost an overall delay of three months in satellite delivery.

Another difficulty that we encountered is also associated with the decision to remove the OBC. We lost control over the kill switch, the existence of which is a requirement for satellite delivery. In case of communication interference, some satellites need to be permanently turned off. Because of a lack of OBC, control over the kill switch was transferred to the COM and, by a command from the GS, the COM can turn the kill switch ON and stop the satellite operation.

As already mentioned, the SPATIUM-I main operation frequency is 467 MHz with a 20% duty cycle. The satellite has other mission modes and a 401-MHz operation frequency. The satellite mission modes are listed in Table 3. Mode M08 is the nominal mode that starts immediately after the satellite is released from the ISS. If any power blackout occurs and the satellite restarts, the operation will resume in M08 mode.

Table 3. SPATIUM-I Mission Modes

Mode	401 MHz		467 MHZ	Power consumption, W
	Rx	Tx (PM)	Tx (SS)	
M00	ON	OFF	OFF	1.08
M01	ON	OFF	OFF	1.08
M02	ON	1min/1min-50%	OFF	3.74
M03	ON	1min/2min-30%	OFF	3.12
M04	ON	1min/4min-20%	OFF	2.10
M05	ON	1min/9min- 10%	OFF	1.61
M06	ON	OFF	1min/1min-50%	3.77
M07	ON	OFF	1min/2min-30%	2.9
M08	ON	OFF	1min/4min-20%	2.03
M09	ON	OFF	1min/9min-10%	1.57
M10	ON	1min/1min-50%	1min/1min-50%	6.35
M11	ON	1min/2min-30%	1min/2min-30%	4.94
M12	ON	1min/4min-20%	1min/4min-20%	3.16
M13	ON	1min/9min- 10%	1min/9min- 10%	2.27

The satellite carries a UHF receiver to be operated with a 401-MHz frequency. The uplink will be done in case we want to change the mission mode. Modes M00–M01 are only reception modes. In these modes, all transmissions are OFF and only the receiver is ON. For others modes M02–M13, the 401-MHz UHF receiver is also always ON. Modes M02–M05 are for performing operations at the 401-MHz downlink frequency. Modes M06–M09 are for performing a 467-MHz frequency downlink. Mission modes M10–M13 allow transmission on both frequencies.

Mode M08 with a 20% duty cycle (2 min ON/ 8 min OFF) is marked with red. This duty cycle has been chosen based on the power budget. A typical 2U CubeSat can generate an average of 2.3 W of power per orbit with 18 solar cells, like SPATIUM-I. A higher-duty cycle will increase the satellite power consumption. Making the ON time shorter is not recommended, considering the time needed for the GS to lock the signal.

During the thermal vacuum test, it was determined that the satellite is heated from the inside out (due to continuous transmission). Mainly, the heat comes from the COM board and battery. Power consumption of the satellite is close to the power generation, and the current required for COM operation is high, which created extra heat inside the battery. The COM heats itself up and also heats the adjacent board (the CSAC board), the main mission board. The battery temperature range is -10º to +50ºC, and the CSAC board is limited by the CSAC device itself by -10º to +70ºC. The maximum observable hot temperature on the COM board was +75ºC (worst case), which could heat the CSAC board up to +65ºC. In the case of the battery, for a CubeSat, overcooling is usually important, but for SPATIUM-I, it is the exact opposite situation, with overheating. To support the system and reduce the heat inside, red satellite panels made of PCB were used (instead of green PCB). The thermo-optical properties of red panels showed a lower coefficient of absorption and lower coefficient of emission than green panels (Table 4). When the ratio of the absorptance to the emittance is low, a satellite tends to have a lower temperature.

Table 4. SPATIUM I Satellite Panels' Thermo-Optical Properties

Material	Solar Absorptance, α_s	Normal Emittance, ε	Ratio of α_s/ε
Green PCB sample #1	0.61	0.94	0.65
Green PCB sample #2	0.63	0.94	0.67
Red PCB sample #1	0.43	0.76	0.57
Red PCB sample #2	0.43	0.75	0.57

To secure all satellite system functionality in case of power generation/consumption, communication and locking time to the GS, minimum acceptable reception time, minimum success requirements, thermal balance onboard the satellite, etc., we chose M08 as the nominal operation mode.

Considering all of the design changes, the SPATIUM-I satellite flight model (FM) model was fabricated. The satellite FM is shown in Figure 5.

Figure 5. SPATIUM I FM model.

3. Ground Station Operation Concept

To provide continuous satellite data reception, the SPATIUM project has GSs in Japan and in Singapore. The project also plans to use the GS network provided by the BIRDS satellite project once the GS equipment becomes available. In 2019, the BIRDS GS network includes 11 GSs. For this network, we will have GSs in Taiwan, Mongolia, Thailand, Nigeria, Ghana, Bhutan, Bangladesh, Malaysia, Philippines, Sri Lanka, and Nepal.

The SPATIUM-I satellite project has two GSs (Japan—uplink, downlink; Singapore—downlink only). Each GS contains antennas operated at the 467-MHz and 401-MHz frequencies. SPATIUM GSs will have a function of data decoding and data comparison with the ground-based referenced CSAC board. The difference between the signals will be defined. The time delay is defined as the time between signal transmission and signal reception. Two different receiving antennas will work on their own frequencies (467 MHz or 401 MHz) (See Figure 6). The main mission signal will be received via the 467-MHz frequency and the first GS antenna. If we need to check the bus system HK data, then the GS sends a signal via a second GS antenna and the satellite will transmit on the 401-MHz frequency or change modes in the 467-MHz frequency if necessary. The second antenna (401 MHz) is basically for the command uplink and some HK data downlink (explained above, in section 2).

With the carrier wave reception, the GS sends a signal through the software defined radio (SDR) to a demodulator. The SDR is used here to convert the frequency to an intermediate frequency that the demodulator can read (IF=45.05 MHz for SPATIUM-I). Each SDR (for 467 MHz and 401 MHz) simultaneously receives a reference 10-MHz clock signal from the ground-based GPS clock.

Since AR2300 cannot provide a time stamp with every single piece of data received by the antenna, a second SDR-Hack RF with a GPS clock time-stamp was implemented. This radio can handle a time stamp, and an I/Q signal is sent for analysis via a computer. The signal delay due to the ionosphere and atmosphere, and the received signal from the satellite will be examined. To derive the signal delay, we need the position of the satellite when the signal is emitted from the satellite, as SPATIUM-I does not carry onboard GPS. Currently, the satellite tracking relies on TLE (two-line element) only; we triangulate the satellite position by receiving the signal at multiple GSs equipped with a GPS-clock and the same SDR (Hack RF radio). We will use multiple GSs provided by the

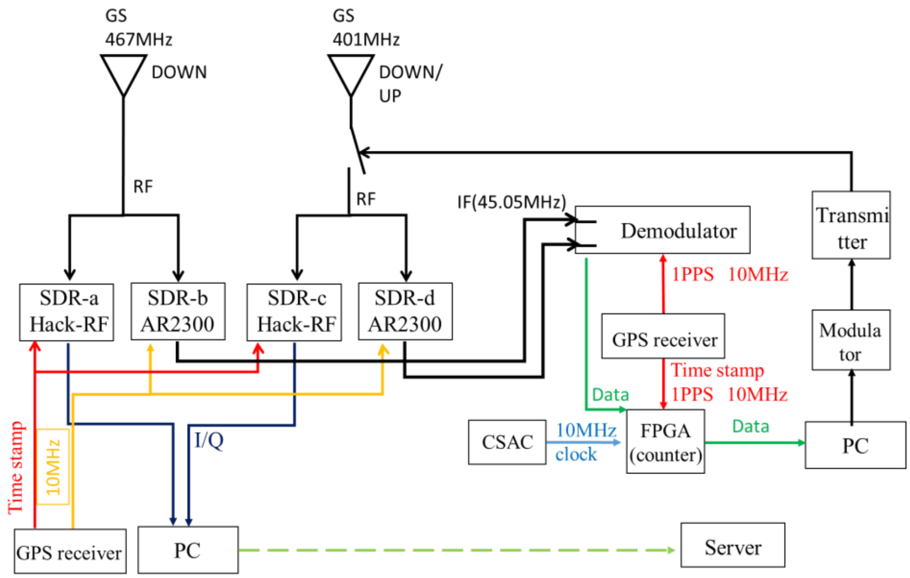

Figure 6. SPATIUM GS system.

BIRDS GS network. The GPS will be implemented on SPATIUM-II and SPATIUM-III.

Both SPATIUM GSs will have modules that reproduce the satellite mission board, as shown in Figure 7. The ground-based CSAC board and FPGA processor are absolutely the same as the ones used for onboard satellite systems. The onboard COM board uses the same FPGA microprocessor to count the CSAC 10MHz signal. The ground-based system is supported by an uninterruptible power supply (UPS) to avoid any power blackout. The ground-based FPGA counter will save the data from the very beginning. In case of a power blackout, the system may lose all the counts

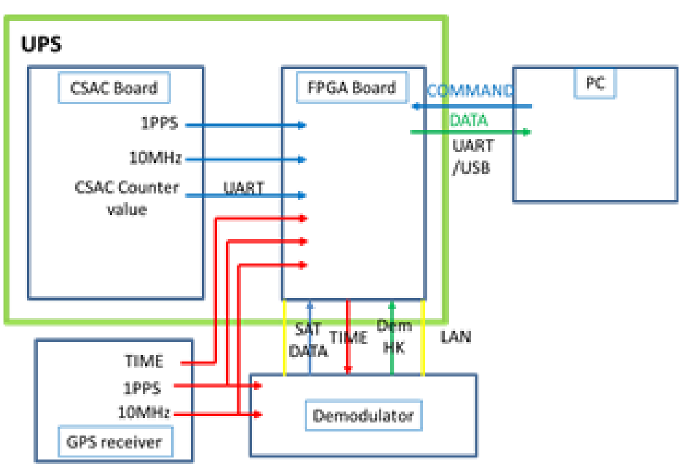

Figure 7. Ground-based reference system.

and, to perform the mission, we will need to start counting from the beginning again.

The referenced CSAC generates a 10-MHz signal, saves data to its own counter, and sends the same data to an FPGA that also counts the data. The signals received from the satellite come through the SDR (AR2300) to the demodulator. The data from the demodulator go to the FPGA. In turn, the FPGA can compare the difference between signals received on the GS and the signal created by the ground-based CSAC device. External ground-based GPS can help with the 10-MHz signal, as a referenced clock, to find out how much of the satellite signal received at the GS was disturbed by the ionosphere.

The SPATIUM-I satellite will have an average lifetime of ~1.5 years. The GS system will analyze and compare data with a ground-based CSAC installed in two countries—Japan and Singapore. For extra mission support, such as satellite tracking and position identification, we can use the BIRDS project's GS network (Cho, 2017).

The SPATIUM-I radio emission has a duty cycle of 20%. The satellite will transmit data for two minutes and keep quiet for eight minutes. With a low elevation angle, we have a shorter pass time; as an average, it is ~9 min. During this time, we are able to receive satellite data only once per pass. With the highest elevation angle, the pass duration can be a maximum of 10–11 min. If we include the time of locking to the GS, we will be able to receive data only once per pass.

During the two minutes of reception, we can receive 120 packets of data if communication has 100% efficiency, ignoring the time necessary to do the carrier and code lock, which can be as long as 60 seconds. This means that we will have 120 data packets from the CSAC counter and 120 data packets from the COM counter after each pass. In one day, one GS will be able to process 600 data packages at maximum. The second GS (Singapore), will support operation and data processing.

For the future global covering (SPATIUM-III) project, we need to have a satellite constellation and a network of GSs to receive data as frequently as possible. Using a single GS and a single satellite on 400 km altitude with a 51.6 degree inclination (same as ISS), we can receive a signal every ~1.5 h. Each communication session is limited in the amount of received data. The limitation here imposes a short time on the satellite's visibility by the GS and the data measurement (satellite signal transmission) is only in one (satellite–GS) direction. If we add one more GS, say in Singapore, then with each satellite pass, the amount of data is doubled and the TEC (Markovici, 2014) is also measured towards two GSs. Thus, by increasing the number of GSs and satellites, and by providing commun ication not only between satellite and GS but also "satellite–satellite" (intersatellite ranging), we can provide a 3D ionosphere map updated in real time.

4. Initial Operation Status

The SPATIUM-I satellite was released from the ISS on October 6, 2018 at 16:45 pm Japan Standard Time (JST). The operation started at 31.5 minutes after the separation. In the first 30 minutes, the satellite transmission was OFF, due to the restriction of transmission near the ISS. During the next 1.5 minutes, the satellite burner circuit was ON, the monopole antennas were deployed, and main mission data transmission automatically started.

The main GS, in Japan, detected a signal on October 7, 2018 at 21.10 pm JST pass by the Spectrum Analyzer (GS antenna was directly connected to the device). During the initial passes, the demodulator could not demodulate the spread spectrum signal. Later, a Doppler shift correction was made on the SDR, instead of the demodulator (initial setting) (Figure 8). Right after changing the Doppler shift correction, we could demodulate the first two packets of data on October 17, 09:09 am JST pass (Figure 9), with some errors. In Table 5, we show the first two packets. The CSAC counter value of the second line (180051 72781537326) contains an error, same for the COM temperature, that is actually around 17 ^{0}C. Figure 10 shows the SS spectrum that the demodulator outputted

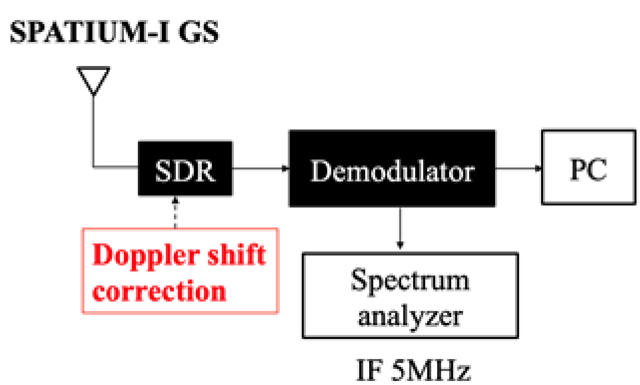

Figure 8. SPATIUM-I GS equipment set-up.

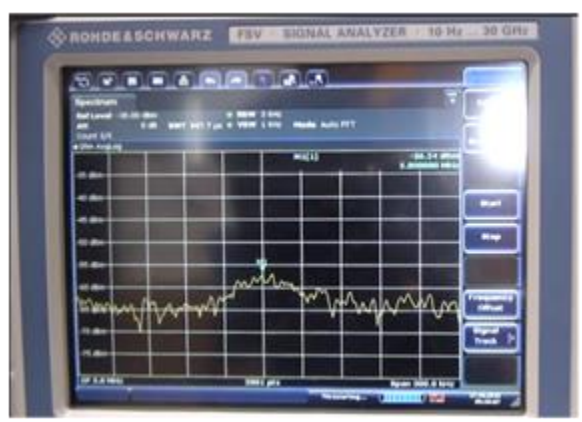

Figure 9. The 5-MHz demodulator channel, during SPATIUM-I data reception.

Table 5. SPATIUM I First Data Packets

SyncMark	SC ID	Op Mode	Frame Counter	CSAC Counter	CSAC 10 MHz counter	CSAC Temp hex	CSAC Temp, ^{0}C
FAF320	00	08	000E1039 2C8A58	00000865 F2660DAF	9233951493551	0494	16.5681
FAF320	00	08	000E1042 2C8A58	003FF79B F7C3582E	180051727815373 26	0493	16.7157

CSAC Volt hex	CSAC Volt, V	COM current hex	COM CUR, A	Batt temp hex	Batt temp, ^{0}C	COM temp hex	COM temp, ^{0}C	Other
0A37	4.2136	1B67	3.6478	08D2	14.4760	F6F1	7447.4740	00
0A36	4.2120	0453	0.5756	08E1	16.3060	F6F7	7448.2060	FF

for the monitoring purpose. After separation from the ISS, the CSAC board powered immediately, to charge the supercapacitor. The CSAC board warm-up time is about two to three minutes. After that, the CSAC counter started counting. The COM board powered in 31.5 minutes after the separation and further antenna deployment. The COM FPGA counter started counting right after that. Therefore, the two counters—the frame counter on the COM FPGA as the main one, and the CSAC counter on the CSAC board as a back-up—have a difference of ~28.965 min. That corresponds to the CSAC board warm-up time and the start of data counting by the COM FPGA 31.5 min after separation from the ISS.

For the first ten days of operation and data reception, 51 data packets were decoded. The data analyzed indicates that all sub-systems are working well. The CSAC 10-MHz counter values are successfully being decoded in most of the cases. The GS demodulator was sometimes malfunctioning, and the GS itself was adjusted by the team for proper operation. Those issues mostly affected on decoding and losing some of the data packets. The operation of the demodulator was adjusted during future operation. Since the SPATIUM-I satellite has a 20% duty cycle, the data comes every ten minutes (two minutes data ON, eight minutes data OFF). We now know that the satellite starts emitting the radio signal at every NN:M6:35, where NN is the hour and M is an integer from 0 to 5.

Presently, most of the data we have been able to decode was obtained while the satellite elevation was low, such as at 20°. We are now trying to increase the amount of data by improving the satellite tracking and the Doppler shift correction. In addition, we noticed a strong background noise around 467 MHz due to the ship communication in the near region, mobile communication, and communication in the Kitakyushu airport, which needs to be suppressed, as it affects the success rate of the data decoding. We have also started working to determine the signal phase to deduce the TEC.

5. Conclusion

The SPATIUM program aims to provide a means of three-dimensional ionosphere mapping to advance planetary science and space weather research. SPATIUM-III will do intersatellite ranging via UHF signals between CubeSats that carries a chip scale atomic clock (GSAC), a GNSS receiver, and an in situ plasma measurement device such as a Langmuir probe. The signal delay between the satellites, and between the satellites and the ground stations (GS) will be used to derive total electron content (TEC) along a signal path. The inverse problem will be solved to derive the vertical and horizontal distribution of electron density. By using a constellation of CubeSats, we can achieve sufficient spatial and temporal resolution to reveal ionosphere dynamics.

The first satellite for the SPATIUM program, SPATIUM-I, carries a CSAC as the main clock source to generate a clock signal with PRN code with spread spectrum modulation. SPATIUM-I tries to demonstrate the use of a CSAC in space by comparing clock counter values with those made by a reference CSAC on the ground. The satellite transmits a signal with a dual-frequency. The signal demodulating at the GS and the signal shift due to the ionosphere can be detected. The GS network's synchronized work and CSAC space operation will be demonstrated.

After a series of verifications mainly via testing, the SPATIUM-I flight model was launched to the International Space Station and released from the Japan Experimental Module on October 6, 2018. The GS successfully received the satellite signal and decoded the spread spectrum modulated signal. The satellite is currently functioning well. Long-term operation to verify CSAC accuracy has begun at the beginning of 2019. Every day, SPATIUM-I has three to four passes over the GS. During every pass, for two minutes (20% duty cycle), we receive data packages every second (360-480 data packages per day or ~130-170k packages per year).

As for today, SPATIUM-I has been in operation for 2.5 years, and since April 2021, we are not receiving data (probably, due to the satellite resets caused by the battery charge). For the end of 2020, SAPTIUM-I demonstrated on-orbit CSAC operation, SS modulated signal reception and demodulation at the ground station via 467 MHz, transmission and reception of the data using 401 MHz frequency. However, time-synchronized multiple ground station operation needs to be improved. The second GS in Singapore started an active operation at the beginning of 2020, and the full success in data comparison was not reached yet (due to the team members relocation, graduation, etc.). As for reading the carrier wave phases (401 MHz and 467 MHz) of a single satellite results, it will be detailed described in the next paper dedicated to the data analysis of SPATIUM-I mission.

We will further improve the GS system to increase the amount of data to be decoded. Identifying the signal phase will also be carried out to deduce the TEC between the satellite and the GS.

The next project that will use CSAC board and further improve the mission is the satellite named KITSUNE, already developed at the Kyushu Institute of Technology and waiting for the launch in 2021.

Acknowledgments

The authors express gratitude to the following entities for their support and contributions: Addnics Corp., the company manufacturer of the SPATIUM I satellite COM board, ground based demodulator, and all support during satellite integration and testing; SAGAMI Electronics Industry Ltd. for the SPATIUM-I satellite bus system manufacturing and all support during testing phase; Infostellar Inc. for the support with a GS network and frequency application process; JAXA for their strong support with a satellite launch and a satellite safety review; Prof. Takuji Ebinuma from Chukyo University for his help with the GPS receiver; and Prof. Mohammad Tariqul Islam and others at the Universiti Kebangsaan Malaysia (UKM) for their research, development and testing of the antenna.

References

Aheieva, K., Rahmatillah, R., Ninagawa, R., Masui, H., Yamauchi, T., Kim, S., Cho, M., Lap, C. C., Siu, T. M., and Holden, L. K. H. (2017a): Space Timing Reference Option for Space Applications Provided by Space Precision Atomic-Clock Timing Utility Mission Satellite “SPATIUM", ISTS 2017-f-003, Matsuyama, Japan. Available at: https://archive.ists.or.jp/upload_pdf/2017-f-003.pdf (accessed Jun. 26, 2021).

Aheieva, K., Rahmatillah, R., Ninagawa, R., Adebolu, I. O., Masui, H., Yamauchi, T., Kim, S., Cho, M., Lap, C. C., Ying, Z., Siu, T. M., Holden, L. K. H. (2017b): CubeSat Mission for Ionosphere Mapping and Weather Forecasting using Chip-Scale Atomic Clock, PIERS 2017, Singapore. Available at: https://www.researchgate.net/profile/Kateryna-Aheieva.

Barros, D., Takahashi, H., Wrasse, C. M., and Figueiredo, C. A. O. B. (2018): Characteristics of Equatorial Plasma Bubbles Observed by TEC Map Based on Ground-based GNSS Receivers over South America, *Ann. Geophys*., Vol. 36, pp. 91–100. doi: https://doi.org/10.5194/angeo-36-91-

2018. Available at: https://angeo.copernicus.org/articles/36/91/2018/ (accessed Jun. 26, 2021).

Cho, M., Jirawattanaphol, A., JGMNB project members, JGMNB partners, and Kurahara, N. (2017): Global Network Operations of CubeSats Constellation, presented at 1st IAA Latin American Symp. on Small Satellites, Mar., Buenos Aires, Argentina. Available at: https://www.unsam.edu.ar/institutos/Colomb/Presentaciones/Session.4/IAA-LA-04-04.pdf (accessed Jun. 26, 2021).

Huang, C.-S., de La Beaujardiere, O., Roddy, P. A., Hunton, D. E., Pfaff, R. F., Valladares, C. E., and Bellenthin, J. O. (2011): Evolution of Equatorial Ionospheric Plasma Bubbles and Formation of Broad Plasma Depletions Measured by the C/NOFS Satellite During Deep Solar Minimum, *J. Geophysical Research*, Vol. 116, A03309. doi:10.1029/2010JA015982. Available at: https://agupubs.onlinelibrary.wiley.com/doi/full/10.1029/2010JA015982 (accessed Jun. 26, 2021).

ISEE (Institute for Space-Earth Environmental Research), Nagoya University: "Project for Solar-Terrestrial Environment Prediction (PSTEP) Models." Available at: https://www.ingentaconnect.com/content/sil/impact/201700002017/00000011//art00003?crawler=true&mimetype=application/pdf (accessed Jun. 26, 2021).

Markovici, M. (2014): Determination of Total Electron Content in the Ionosphere Using GPS Technology, Geonauka, Vol. 2, No. 2. Available at: http://scindeks-clanci.ceon.rs/data/pdf/2334-8119/2014/2334-81191404001M.pdf (accessed Jun. 26, 2021).

NOAA (National Oceanic and Atmospheric Administration), National Weather Service (NWS) Space Weather Prediction Center: "WAM-IPE Model." Available at: https://www.swpc.noaa.gov/products/aurora-3-day-forecast (accessed Jun. 26, 2021).

Tejumola, T. R., Birds Project Members, Birds Partners, Maeda, G., Kim, S., Masui, H., and Cho, M. (2017): Overview of Joint Global Multi-Nation Birds Satellite Project, ISTS 2017-f-015, Matsuyama, Japan. Available at: https://www.researchgate.net/publication/322567870_Overview_of_Joint_Global_Multi-Nation_Birds_Satellite_Project (accessed Jun. 26, 2021).

Tokunaga, Y. and Cho, M. (2017): Challenges in the Development of the Backplane-type Bus for 1U CubeSat, ISTS 2017-f-018, Matsuyama, Japan. Available at: https://www.researchgate.net/publication/317426406_Challenges_in_bus_system_development_of_1U_CubeSat (accessed Jun. 26, 2021).